

LETTERS

Reconstruction of the history of anthropogenic CO₂ concentrations in the ocean

S. Khatiwala¹, F. Primeau² & T. Hall³

The release of fossil fuel CO₂ to the atmosphere by human activity has been implicated as the predominant cause of recent global climate change¹. The ocean plays a crucial role in mitigating the effects of this perturbation to the climate system, sequestering 20 to 35 per cent of anthropogenic CO₂ emissions^{2–4}. Although much progress has been made in recent years in understanding and quantifying this sink, considerable uncertainties remain as to the distribution of anthropogenic CO₂ in the ocean, its rate of uptake over the industrial era, and the relative roles of the ocean and terrestrial biosphere in anthropogenic CO₂ sequestration. Here we address these questions by presenting an observationally based reconstruction of the spatially resolved, time-dependent history of anthropogenic carbon in the ocean over the industrial era. Our approach is based on the recognition that the transport of tracers in the ocean can be described by a Green's function, which we estimate from tracer data using a maximum entropy deconvolution technique. Our results indicate that ocean uptake of anthropogenic CO₂ has increased sharply since the 1950s, with a small decline in the rate of increase in the last few decades. We estimate the inventory and uptake rate of anthropogenic CO₂ in 2008 at 140 ± 25 Pg C and 2.3 ± 0.6 Pg C yr⁻¹, respectively. We find that the Southern Ocean is the primary conduit by which this CO₂ enters the ocean (contributing over 40 per cent of the anthropogenic CO₂ inventory in the ocean in 2008). Our results also suggest that the terrestrial biosphere was a source of CO₂ until the 1940s, subsequently turning into a sink. Taken over the entire industrial period, and accounting for uncertainties, we estimate that the terrestrial biosphere has been anywhere from neutral to a net source of CO₂, contributing up to half as much CO₂ as has been taken up by the ocean over the same period.

A key challenge for estimating anthropogenic CO₂ (C_{ant}) in the ocean is that C_{ant} is not a directly measurable quantity. Existing estimates of C_{ant} are thus based on indirect techniques, such as so-called 'back calculation' methods that attempt to separate the small anthropogenic perturbation (of the order of a few per cent) from the large background distribution of carbon by correcting the measured total dissolved inorganic carbon (DIC) concentration for changes due to biological activity and air–sea disequilibrium^{5,6}. The recent availability of a high quality, global tracer data set⁷ and significant improvements in methodology, notably the development of the ΔC* approach⁸, made it possible to apply these ideas, and led to one of the first observationally based global estimates of the distribution of C_{ant} in the ocean². Although a major advance in our understanding of C_{ant} in the ocean, it has been suggested that this estimate suffers from a number of biases and limitations^{9–11}, one of them being that it provides only a snapshot for the mid-1990s.

Our method for estimating anthropogenic CO₂ builds on previous work^{11,12}, but extends it in several significant ways. Following previous

studies, we exploit the fact that the anthropogenic perturbation can be treated as a conservative tracer¹³ transported by ocean circulation from the surface mixed layer into the interior. The transport of water that carries C_{ant} into the interior ocean involves considerable dispersion and mixing of water masses of different ages and of different surface origin. Anthropogenic CO₂ at an interior location **x** and at time *t* is therefore related to its history in the surface mixed layer, C_{ant}^s, through a convolution equation involving a kernel, \mathcal{G} , which partitions each water parcel according to where and when it was last in contact with the sea surface:

$$C_{\text{ant}}(\mathbf{x}, t) = \int d\mathbf{x}' \int_{1765}^t dt' C_{\text{ant}}^s(\mathbf{x}', t') \mathcal{G}(\mathbf{x}, t; \mathbf{x}', t') \quad (1)$$

The time integral in equation (1) is over the industrial era and the space integral is over the whole ocean surface. The kernel, $\mathcal{G}(\mathbf{x}, t; \mathbf{x}', t')$, is an intrinsic property of the ocean circulation and not of any particular tracer. As such, it can be used to propagate the surface boundary condition of any conservative tracer into the full three-dimensional concentration field. We exploit this fact by using a suite of well sampled oceanic tracers such as chlorofluorocarbons, natural ¹⁴C, temperature, and salinity from the GLODAP and World Ocean Atlas databases (see Methods), to provide constraints analogous to equation (1) from which we deconvolve \mathcal{G} . We recognize that there is no single tracer that perfectly emulates the C_{ant} transient, necessitating the use of multiple tracers with distinct time histories to constrain \mathcal{G} . To regularize the under-determined deconvolution problem, we use a maximum entropy method¹⁴ which is well suited for problems with positive kernels. We note that the C_{ant} estimated via equation (1) is relatively insensitive to errors in \mathcal{G} as the latter only appears via a convolution¹².

Apart from \mathcal{G} , we need an estimate of C_{ant}^s in order to apply equation (1) to compute C_{ant}. We obtain this boundary condition from the known atmospheric CO₂ history by requiring that the rate of change of the inventory of C_{ant} (obtained by integrating equation (1) over the volume of the ocean) must, by mass conservation, be equal to its net flux into the ocean. The air–sea flux of C_{ant} is proportional to the change in surface disequilibrium of CO₂ (see Methods). To make further progress, we exploit the empirical result from ocean carbon cycle models that the change in disequilibrium is, to a very good approximation, proportional to the (known) anthropogenic perturbation in the atmospheric partial pressure of CO₂, p_{CO₂}. To estimate the unknown, spatially variable proportionality constant, we combine the above constraint with the requirement that our solution match observed p_{CO₂} values averaged over a discrete set of surface patches, subject to the CO₂-system equilibrium chemistry. Once the proportionality constants are known, the history of C_{ant} on each surface patch is readily obtained.

We note that our inversion method provides improvements to reduce the three main biases of most previous techniques¹⁰, namely:

¹Lamont-Doherty Earth Observatory of Columbia University, Palisades, New York 10964, USA. ²Department of Earth System Science, University of California, Irvine, California 92697, USA. ³NASA Goddard Institute for Space Studies, 2880 Broadway, New York, New York 10025, USA.

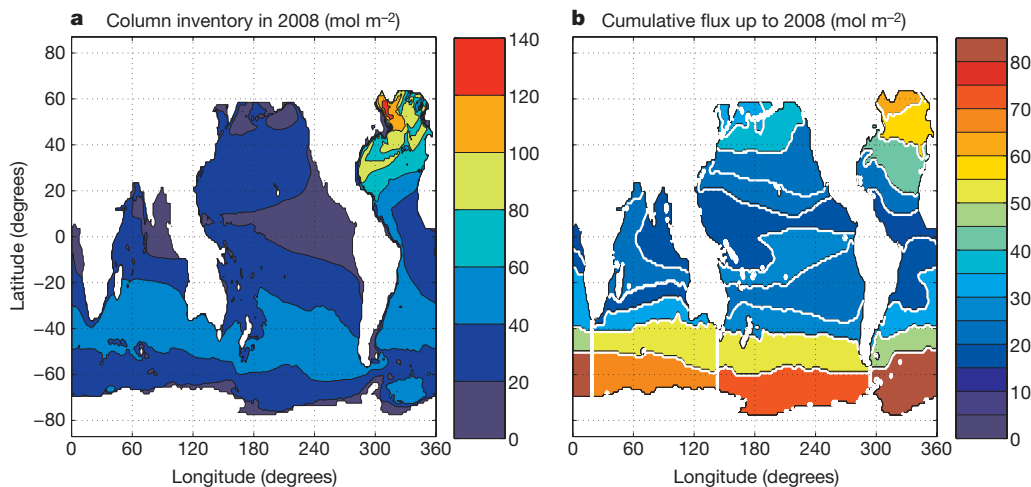


Figure 1 | Anthropogenic carbon in the ocean. **a**, Column inventory of C_{ant} in the ocean in 2008; the total inventory of C_{ant} in 2008 was ~ 140 Pg C. **b**, Cumulative C_{ant} uptake intensity up to 2008 partitioned according to surface region. The white lines delineate the 26 surface patches used in the inversion. To estimate the uncertainties quoted in the text, we repeated the analysis by randomly sampling the various parameters used in the inversion from a uniform distribution centred about the observed value of the

(1) the air–sea disequilibrium is allowed to evolve and is estimated by solving a nonlinear optimization problem, (2) the mixing of waters of different ages is accounted for by using multiple transient and steady tracers to constrain the age distribution, and (3) the mixing of different end-member water types is accounted for by constraining \mathcal{G} using multiple steady and transient tracers. Tests using tracers simulated with a global ocean circulation model show that our method is able to successfully recover the complex spatial distribution of C_{ant} in the model with a maximum error in the column inventory of $\sim 2 \text{ mol m}^{-2}$ and an error in the global inventory of less than 2% (Supplementary Information).

Using our new inverse method, we have reconstructed the first three-dimensional, time-varying, history of anthropogenic carbon in the ocean from AD 1765 to AD 2008. Figure 1a shows the column inventory of C_{ant} in 2008. The total inventory in that year was $\sim 140 \pm 25$ Pg C. This estimate excludes the Arctic Ocean and marginal seas not covered by the GLODAP database. Using a recent estimate based on CFC-11 for the former¹⁵, and an area scaling approach for the latter², would increase our estimate of the global inventory by ~ 11 Pg C. We have also partitioned this inventory according to where at the surface the anthropogenic CO_2 penetrated the ocean. As is evident from Fig. 1b, the high latitude oceans, driven by intermediate and deep water formation, constitute the most intense sinks of C_{ant} . In particular, the Southern Ocean is by far the largest conduit by which anthropogenic CO_2 enters the ocean: roughly 40% of the C_{ant} residing in the ocean in 2008 entered the ocean south of 40°S .

It is useful to compare our result for 1994 to previous estimates that are available for that year. The inventory estimated using the so-called ΔC^* method² for 1994 is 106 ± 21 Pg C. The 1994 inventory estimated using the transit-time distribution (TTD) method¹¹ is 107 Pg C, with a range of 94–121 Pg C. Both estimates are consistent with our 1994 estimate of 114 ± 22 Pg C. However, the previous TTD-based estimate includes a 20% downward correction for the fact that air–sea disequilibrium was incorrectly treated as being constant. Such a correction, based on model simulations, is not necessary for our estimate because our inverse method explicitly accounts for changing air–sea disequilibrium. The spatial distribution we obtain is quite different from that obtained with the ΔC^* method, particularly in the Southern Ocean. Relative to the ΔC^* -based estimate, our estimate of C_{ant} , like the TTD-based estimate, is generally lower in the upper ocean and higher in the deep ocean¹¹. Two key aspects of

the ΔC^* method are the use of a single tracer age to characterize transport and the assumption of constant disequilibrium. These give rise to competing biases¹⁰ that largely cancel out, leading to the close, but fortuitous, agreement between our estimate of the total inventory and that derived using the ΔC^* method.

Figure 2 shows the uptake history over the industrial era (AD 1765 to AD 2008) computed from the time-varying inventory. (The corresponding space- and time-varying change in surface disequilibrium of CO_2 driving this uptake is also estimated by our inversion method.) There has been a sharp increase in ocean uptake since the 1950s in response to a higher growth rate of atmospheric CO_2 , although the rate of increase has decreased somewhat in the last few decades. Our estimated uptake rate for the 1990s, $2.0 \pm 0.6 \text{ Pg C yr}^{-1}$, agrees well with the IPCC consensus estimate based on independent methods⁴ (Fig. 2 and Table 1).

Our work has important implications for the terrestrial carbon budget, here computed as a residual between the main fossil fuel source and the ocean and atmosphere sinks. (Including the highly

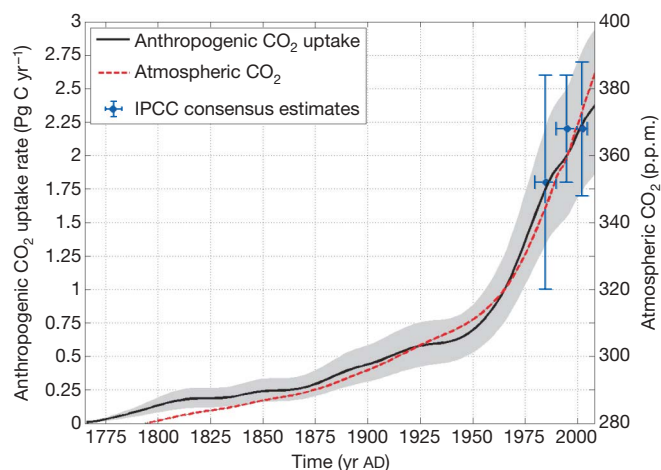


Figure 2 | Anthropogenic carbon uptake rate from 1765 to 2008 (black solid line). The shaded area represents the error envelope (see Fig. 1 legend). Also shown are the decadal average uptake rates adopted by the IPCC fourth-assessment report (AR4)⁴ (blue circles; vertical error bars are ± 1 s.d. and horizontal error bars span the averaging period of years) and the atmospheric CO_2 mixing ratio²⁹ used for the inversion (red dashed line).

Table 1 | Decadal mean ocean and land uptake rates of C_{ant}

Period	Ocean (Pg C yr ⁻¹)	Land (Pg C yr ⁻¹)	Ocean – AR4 (Pg C yr ⁻¹)	Land – AR4 (Pg C yr ⁻¹)
1980s	1.8 (1.3–2.3)	0.3 (–0.3 to 0.8)	1.8 (1.0–2.6)	0.3 (–0.6 to 1.2)
1990s	2.0 (1.4–2.6)	1.1 (0.5–1.8)	2.2 (1.8–2.6)	1.0 (0.4–1.6)
2000s	2.3 (1.7–2.9)	1.1 (0.4–1.8)	2.2 (1.8–2.6)†	1.3 (0.7–1.9)†

Columns 1 and 2 show uptake rates from this work; columns 3 and 4 show corresponding values adopted by the IPCC AR4. For the current decade, the average is over 2000–06.

† IPCC ocean and land uptake values derived from a numerical ocean model simulation^{17,19}.

uncertain source due to changes in land use¹⁶ provides a different perspective; Supplementary Fig. 3.) There remains considerable uncertainty regarding the relative partitioning of anthropogenic emissions between the ocean and land biosphere³. Our time-evolving estimate of the ocean uptake provides a more precise and detailed view of the land sink. Table 1 compares our estimates for the uptake rate of C_{ant} by the land biosphere with other estimates^{4,17}. There is generally good agreement between the two, although the latter only go back to the 1980s, whereas our approach covers the entire industrial period. Figure 3 shows the evolution of the various sources and sinks of anthropogenic CO₂ between AD 1765 and AD 2005. Our results indicate that the terrestrial biosphere was a source of C_{ant} until the 1940s, roughly in line with previous model-based estimates^{3,18}, after which it turned into a sink of anthropogenic CO₂. Taken over the entire industrial period, and accounting for uncertainties, we estimate that the terrestrial biosphere has been anywhere from neutral to a net source of CO₂, contributing up to half as much C_{ant} as has been taken up by the ocean over the same period.

One potential source of error we have neglected is variability in ocean circulation, especially long-term trends. Such variability, however, remains poorly constrained, and its impact on anthropogenic CO₂ uptake is still debated. For example, ocean models show a slight decline in the rate-of-growth of C_{ant} uptake by the Southern Ocean over the past few decades due to an increase in the strength of the meridional overturning circulation (MOC) in response to strengthened westerly winds^{19,20}. However, a recent study²¹ finds no observational evidence for such a change in the MOC, suggesting that the simulated changes in the MOC and uptake may be an artefact of the eddy-parametrization used in coarse-resolution ocean models^{21,22}. Nevertheless, it is useful to place these modelled changes within the context of our inverse calculations, which assume a cyclo-stationary circulation. The simulated decrease¹⁹, of ~ 0.08 Pg C yr⁻¹ per decade between 1981 and 2004, would imply a reduction in C_{ant} uptake of roughly 2.1 Pg C over that period (equivalent to a 1 p.p.m. increase in atmospheric CO₂ concentration). This

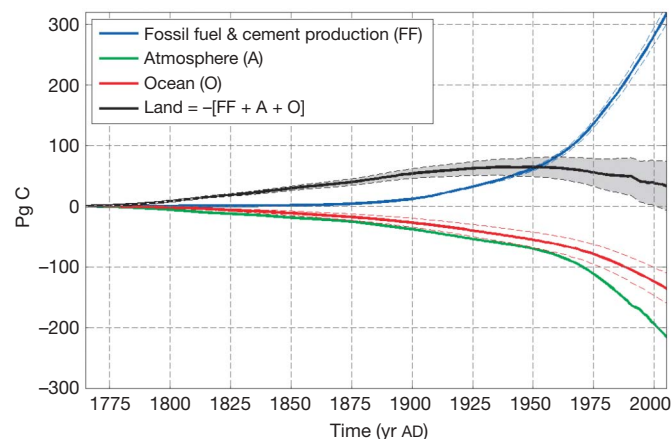


Figure 3 | Evolution of anthropogenic CO₂ sources and sinks between 1765 and 2005. Fossil fuel burning³⁰ (including a small contribution from cement production) is the only source considered here, and is shown as positive values. Sinks, shown as negative values, include the atmosphere, ocean, and land biosphere. Error envelope (as in Fig. 1 legend), indicated by broken lines and the shaded area, includes a 5% uncertainty in fossil fuel emissions¹⁷.

value should be compared with a total ocean uptake of 46 ± 6 Pg C over the same period, as estimated by our inverse method (17.5 ± 2.5 Pg C for the Southern Ocean)—that is, a 5% reduction in the global ocean sink of anthropogenic CO₂, but still well within the uncertainty of our purely data-based estimate.

To conclude, we have presented an observationally based estimate of the time-evolving distribution of anthropogenic CO₂ in the ocean over the industrial era. Unlike other recent inverse calculations²³, we do not rely on an ocean model for transport information. Errors in transport simulated by such models^{23–25} are a large source of uncertainty in estimates of C_{ant} based on those inverse calculations. Instead, we constrain the transport by using tracer observations. Our results can thus be used to assess and improve global ocean biogeochemical models, initialize high-resolution simulations, and provide boundary conditions for atmospheric inversions of anthropogenic sources and sinks.

METHODS SUMMARY

The combined GLODAP/WOA05 databases (see Methods) provide six constraints, one for each tracer, of the form: $C(\mathbf{x}, t) = \int d\mathbf{x}' \int_{-\infty}^t dt' e^{-\lambda(t-t')} C(\mathbf{x}', t') \mathcal{G}(\mathbf{x}, t; \mathbf{x}', t')$, where C is the observed tracer concentration, and λ its radioactive decay rate (non-zero only for ¹⁴C). To reduce the indeterminacy, we assume that the ocean circulation is stationary except for a cyclo-stationary seasonal cycle and we discretize the sea surface position variable, \mathbf{x}' , into a discrete set of 26 surface patches (Fig. 1b). With these assumptions, the kernel for each interior position, \mathbf{x} , can be written as a discrete function, $\mathcal{G}(i, k, m)$ in which i is the surface-patch index, and k and m are respectively the number of years since, and the month when, the water was last in the surface mixed layer. To further regularize the deconvolution, we used a maximum entropy approach in which we maximize an entropy functional, $J[\mathcal{G}] = - \sum_{i,k,m} \mathcal{G}(i, k, m) \log \frac{\mathcal{G}(i,k,m)}{\mathcal{M}(i,k,m)}$, subject to the discretized tracer constraints. \mathcal{M} is a prior estimate of \mathcal{G} , which we take to be an analytical solution to the one-dimensional advection–diffusion equation known as the inverse Gaussian²⁶. Simulations in ocean general circulation models²⁷ show that the inverse Gaussian form captures well the general characteristics of \mathcal{G} . The inverse Gaussian is characterized by two parameters, a mean age Γ and width Δ . Consistent with tracer observations^{26,28}, we set $\Delta = \Gamma$, which leaves us with one free parameter. To specify Γ , we make it a function of depth, increasing linearly from 10 yr in the surface layer to 2,000 yr in the deepest layer. The resulting variational problem is solved using the method of Lagrange multipliers, and yields a solution of the form (shown for clarity using the continuous time variables):

$$\mathcal{G}(\mathbf{x}, t; i) = \mathcal{M}(\mathbf{x}, t; i) e^{-\sum_j \alpha_j(\mathbf{x}) C_j^o(t_j - t; i) e^{-\lambda_j t}}$$

where $\alpha_j(\mathbf{x})$ is the Lagrange multiplier required to enforce the j th observational constraint. The above yields a system of nonlinear algebraic equations for the Lagrange multipliers, which we solve using standard methods.

Full Methods and any associated references are available in the online version of the paper at www.nature.com/nature.

Received 14 May; accepted 15 September 2009.

- Solomon, S. et al. (eds) *Climate Change 2007 — The Physical Science Basis* (Cambridge Univ. Press, 2007).
- Sabine, C. L. et al. The ocean sink for anthropogenic CO₂. *Science* **305**, 367–371 (2004).
- Houghton, R. A. Balancing the global carbon budget. *Annu. Rev. Earth Planet. Sci.* **35**, 313–347 (2007).
- Denman, K. L. et al. in *Climate Change 2007 — The Physical Science Basis* (eds Solomon, S. et al.) 499–587 (Cambridge Univ. Press, 2007).
- Brewer, P. G. Direct measurements of the oceanic CO₂ increase. *Geophys. Res. Lett.* **5**, 997–1000 (1978).
- Chen, C.-T. & Millero, F. J. Gradual increase of oceanic CO₂. *Nature* **277**, 205–206 (1979).
- Key, R. M. et al. A global ocean carbon climatology: results from GLODAP. *Glob. Biogeochem. Cycles* **18**, doi:10.1029/2004GB002247 (2004).
- Gruber, N., Sarmiento, J. L. & Stocker, T. F. An improved method for detecting anthropogenic CO₂ in the oceans. *Glob. Biogeochem. Cycles* **10**, 809–837 (1996).
- Wallace, D. W. R. Ocean measurements and models of carbon sources and sinks. *Glob. Biogeochem. Cycles* **15**, 3–10, doi:10.1029/2000GB001354 (2001).
- Matsumoto, K. & Gruber, N. How accurate is the estimation of anthropogenic carbon in the ocean? An evaluation of the ΔC^* method. *Glob. Biogeochem. Cycles* **19**, doi:10.1029/2004GB002397 (2005).

11. Waugh, D. W., Hall, T. M., McNeil, B. I., Key, R. M. & Matear, R. J. Anthropogenic CO₂ in the oceans estimated using transit-time distributions. *Tellus B* **58**, 376–390 (2006).
12. Hall, T. M., Haine, T. W. N. & Waugh, D. W. Inferring the concentration of anthropogenic carbon in the ocean from tracers. *Glob. Biogeochem. Cycles* **16**, doi:10.1029/2001GB001835 (2002).
13. Sarmiento, J. L., Orr, J. C. & Siegenthaler, U. A perturbation simulation of CO₂ uptake in an ocean general circulation model. *J. Geophys. Res.* **97**, 3621–3645 (1992).
14. Tarantola, A. *Inverse Problem Theory and Methods for Model Parameter Estimation* (Society for Industrial and Applied Mathematics, 2005).
15. Tanhua, T. *et al.* Ventilation of the Arctic Ocean: mean ages and inventories of anthropogenic CO₂ and CFC-11. *J. Geophys. Res.* **114**, doi:10.1029/2008JC004868 (2009).
16. Houghton, R. A. *Carbon Flux to the Atmosphere from Land-Use Changes 1850–2005* (Carbon Dioxide Information Analysis Center, Oak Ridge National Laboratory, 2008); (<http://cdiac.ornl.gov/trends/landuse/houghton/1850–2005.txt>).
17. Canadell, J. G. *et al.* Contributions to accelerating atmospheric CO₂ growth from economic activity, carbon intensity and efficiency of natural sinks. *Proc. Natl Acad. Sci. USA* **104**, 18866–18870 (2007).
18. Joos, F., Meyer, R., Bruno, M. & Leuenberger, M. The variability in the carbon sinks as reconstructed for the last 1000 years. *Geophys. Res. Lett.* **26**, 1437–1440 (1999).
19. Le Quéré, C. *et al.* Saturation of the Southern Ocean CO₂ sink due to recent climate change. *Science* **316**, doi:10.1126/science.1136188 (2007).
20. Lovenduski, N. S., Gruber, N., Doney, S. C. & Lima, I. D. Enhanced CO₂ outgassing in the Southern Ocean from a positive phase of the Southern Annular Mode. *Glob. Biogeochem. Cycles* **21**, doi:10.1029/2006GB002900 (2007).
21. Böning, C. W., Dispert, A., Visbeck, M., Rintoul, S. & Schwarzkopf, F. U. Response of the Antarctic Circumpolar Current to recent climate change. *Nature Geosci.* **1**, 864–869 (2008).
22. Zickfeld, K., Fyfe, J., Saenko, O. A., Eby, M. & Weaver, A. J. Response of the global carbon cycle to human-induced changes in the Southern Hemisphere winds. *Geophys. Res. Lett.* **34**, doi:10.1029/2006GL028797 (2007).
23. Mikaloff Fletcher, S. E. *et al.* Inverse estimates of anthropogenic CO₂ uptake, transport, and storage by the ocean. *Glob. Biogeochem. Cycles* **20**, doi:10.1029/2005GB002530 (2006).
24. Matsumoto, K. *et al.* Evaluation of ocean carbon cycle models with data-based metrics. *Geophys. Res. Lett.* **31**, doi:10.1029/2003GL018970 (2004).
25. Cao, L. *et al.* The role of ocean transport in the uptake of anthropogenic CO₂. *Biogeosciences* **6**, 375–390 (2009).
26. Waugh, D. W., Haine, T. W. & Hall, T. M. Transport times and anthropogenic carbon in the subpolar North Atlantic Ocean. *Deep Sea Res. I* **51**, 1475–1491 (2004).
27. Khatiwala, S., Visbeck, M. & Schlosser, P. Age tracers in an ocean GCM. *Deep Sea Res. I* **48**, 1423–1441 (2001).
28. Hall, T. M., Waugh, D. W., Haine, T. W. N., Robbins, P. E. & Khatiwala, S. Estimates of anthropogenic carbon in the Indian Ocean with allowance for mixing and time-varying air-sea CO₂ disequilibrium. *Glob. Biogeochem. Cycles* **18**, doi:10.1029/2003GB002120 (2004).
29. *Atmospheric Trace Gases: Carbon Dioxide* (Carbon Dioxide Information Analysis Center, Oak Ridge National Laboratory, 2009); (<http://cdiac.ornl.gov/trends/co2>).
30. Boden, T. A., Marland, G. & Andres, R. J. *Global, Regional, and National Fossil-fuel CO₂ Emissions* doi:10.3334/CDIAC/00001 (Carbon Dioxide Information Analysis Center, Oak Ridge National Laboratory, 2009); (http://cdiac.ornl.gov/trends/emis/tre_glob.html).

Supplementary Information is linked to the online version of the paper at www.nature.com/nature.

Acknowledgements This work was supported by US NSF grants OCE 06-23366 (to S.K. and T.H.) and OCE 07-26871 (to F.P.).

Author Contributions All authors contributed extensively to the work presented in this paper.

Author Information Reprints and permissions information is available at www.nature.com/reprints. Correspondence and requests for materials should be addressed to S.K. (spk@ldeo.columbia.edu).

METHODS

Observational data used for deconvolution of \mathcal{G} . The tracers we use for the deconvolution include gridded fields of CFC-11, CFC-12, and natural ^{14}C from the GLODAP database⁷, and temperature, salinity, oxygen and phosphate from the World Ocean Atlas 2005^{31–34} (WOA05). While ^{14}C is not a conservative tracer, its radioactive decay rate is known and can be accounted for in the convolution. Oxygen and phosphate are also non-conservative because of the remineralization of organic matter that consumes oxygen and releases phosphate. However, the two tracers can be combined into a conservative tracer³⁵ $\text{PO}_4^* (\equiv \text{PO}_4 + \text{O}_2/175)$. In general, temperature, salinity and PO_4^* provide information about the mixing of different end-member water types, while the CFCs and ^{14}C provide surface-to-interior transit-time information.

To construct the surface boundary conditions for CFC-11 and CFC-12, we scaled the known atmospheric history of those tracers³⁶ to the measured surface concentration, hence approximately accounting for undersaturation of these gases in the mixed layer^{37–39}. For the other tracers, we use a monthly mean climatology. Gas-transfer coefficients⁴⁰ were averaged over each surface patch.

We note that our inversion methodology does not require observations of carbon in the ocean interior, but does utilize surface carbon measurements (see below).

Computation of surface boundary condition for C_{ant} . To compute the boundary condition for C_{ant} , we require that the instantaneous rate of change of inventory of C_{ant} must, by mass conservation, be equal to its net flux into the ocean:

$$\frac{d}{dt} \int_{\text{volume}} dx \int_{\text{surface}} dx' \int_{1765}^t dt' C_{\text{ant}}^s(\mathbf{x}', t') \mathcal{G}(\mathbf{x}, t; \mathbf{x}', t') = \int F(\mathbf{x}', t) dx' \quad (2)$$

The air-sea flux of anthropogenic CO_2 is in turn given by

$$F(\mathbf{x}', t') = -k(\mathbf{x}') [\delta p_{\text{CO}_2}(\mathbf{x}', t') - \delta p_{\text{CO}_2}^{\text{atm}}(t')] \equiv -k(\mathbf{x}') \delta \Delta p_{\text{CO}_2}(\mathbf{x}', t') \quad (3)$$

where k is a gas-transfer coefficient, Δ represents the air-sea difference, and δ represents the anthropogenic perturbation. This equation shows that the flux is proportional to the change in surface disequilibrium of CO_2 . We further exploit the empirical result from ocean carbon cycle models (Supplementary Information) that the change in disequilibrium is, to a very good approximation, proportional to the (known) anthropogenic perturbation in atmospheric p_{CO_2} :

$$\delta \Delta p_{\text{CO}_2}(\mathbf{x}', t') \approx \varepsilon(\mathbf{x}') \delta p_{\text{CO}_2}^{\text{atm}}(t') \quad (4)$$

where ε is the (unknown) proportionality constant. This allows us to recast the RHS of equation (2) in terms of ε . The LHS can similarly be recast by relating the dissolved inorganic carbon (DIC) concentration in surface waters to the partial

pressure of CO_2 via the equilibrium chemistry for the CO_2 system in sea water. Denoting this equilibrium as $\text{DIC} = f(p_{\text{CO}_2})$, we have:

$$C_{\text{ant}}^s(\mathbf{x}', t') \approx f(p_{\text{CO}_2}(\mathbf{x}', 1765) + (1 + \varepsilon(\mathbf{x}')) \delta p_{\text{CO}_2}^{\text{atm}}(t')) - f(p_{\text{CO}_2}(\mathbf{x}', 1765)) \quad (5)$$

The unknown pre-industrial surface p_{CO_2} appearing in the above equation is given by:

$$p_{\text{CO}_2}(\mathbf{x}', 1765) \approx p_{\text{CO}_2}(\mathbf{x}', t_{\text{obs}}) - (1 + \varepsilon(\mathbf{x}')) \delta p_{\text{CO}_2}^{\text{atm}}(t_{\text{obs}})$$

where $p_{\text{CO}_2}(\mathbf{x}', t_{\text{obs}})$ is the measured value of p_{CO_2} at time t_{obs} . We take these from a recently compiled database of global surface p_{CO_2} observations⁴¹. In this manner, the constraint equation (2) can be written entirely in terms of a single set of unknowns, the $\varepsilon(\mathbf{x}')$. In practice, since equation (2) must hold at every instant, we discretize in time with annual resolution and average in space over a discrete set of surface patches to obtain a set of nonlinear equations for the ε_i that we solve using standard nonlinear least squares.

31. Locarnini, R. A. *et al.* *World Ocean Atlas 2005 Vol. 1, Temperature* (NOAA Atlas NESDIS 61, US Government Printing Office, 2006).
32. Antonov, J. I., Locarnini, R. A., Boyer, T. P., Mishonov, A. V. & Garcia, H. E. *World Ocean Atlas 2005 Vol. 2, Salinity* (NOAA Atlas NESDIS 62, US Government Printing Office, 2006).
33. Garcia, H. E., Locarnini, R. A., Boyer, T. P. & Antonov, J. I. *World Ocean Atlas 2005 Vol. 3, Dissolved Oxygen, Apparent Oxygen Utilization, and Oxygen Saturation* (NOAA Atlas NESDIS 63, US Government Printing Office, 2006).
34. Garcia, H. E., Locarnini, R. A., Boyer, T. P. & Antonov, J. I. *World Ocean Atlas 2005 Vol. 4, Nutrients (Phosphate, Nitrate, Silicate)* (NOAA Atlas NESDIS 64, US Government Printing Office, 2006).
35. Broecker, W. S. *et al.* How much deep water is formed in the Southern Ocean? *J. Geophys. Res.* **103**, 15833–15844 (1998).
36. Walker, S. J., Weiss, R. F. & Salameh, P. K. Reconstructed histories of the annual mean atmospheric mole fractions for the halocarbons CFC11, CFC-12, CFC113 and carbon tetrachloride. *J. Geophys. Res.* **105**, 14285–14296 (2000).
37. Smethie, W. M. & Fine, R. A. Rates of North Atlantic Deep Water formation calculated from chlorofluorocarbon inventories. *Deep Sea Res.* **148**, 189–215 (2001).
38. Rhein, M. *et al.* Labrador Sea Water: pathways, CFC inventory, and formation rates. *J. Phys. Oceanogr.* **32**, 648–665 (2002).
39. Lo Monaco, C., Goyet, C., Metzl, N., Poisson, A. & Touratier, F. Distribution and inventory of anthropogenic CO_2 in the Southern Ocean: comparison of three data-based methods. *J. Geophys. Res.* **110**, doi:10.1029/2004JC002571 (2005).
40. Sweeney, C. *et al.* Constraining global air-sea gas exchange for CO_2 with recent bomb ^{14}C measurements. *Glob. Biogeochem. Cycles* **21**, doi:10.1029/2006GB002784 (2007).
41. Takahashi, T. *et al.* Climatological mean and decadal change in surface ocean p_{CO_2} , and net sea-air CO_2 flux over the global oceans. *Deep Sea Res.* **11** **56**, doi:10.1016/j.dsr2.2008.12.009 (2009).